Title

A Readily Scalable, Clinically Demonstrated, Antibiofouling Zwitterionic Surface Treatment for Implantable Medical Devices

Journal

Advanced Materials, 34(20)

ISSN

0935-9648

Authors

McVerry, Brian
Polasko, Alexandra
Rao, Ethan
et al.

Publication Date

2022-05-01

DOI

10.1002/adma.202200254

Peer reviewed

Published in final edited form as:

Adv Mater. 2022 May ; 34(20): e2200254. doi:10.1002/adma.202200254.

A Readily Scalable, Clinically Demonstrated, Antibiofouling Zwitterionic Surface Treatment for Implantable Medical Devices

Brian McVerry,
Department of Chemistry and Biochemistry, University of California, Los Angeles, CA 90095, USA

Silq Technologies, Corp., Los Angeles, CA 90025, USA

Alexandra Polasko,
Department of Civil and Environmental Engineering, University of California, Los Angeles, CA 90095, USA

Ethan Rao,
Department of Chemistry and Biochemistry, University of California, Los Angeles, CA 90095, USA

Silq Technologies, Corp., Los Angeles, CA 90025, USA

Reihaneh Haghniaz,
Center for Minimally Invasive Therapeutics (C-MIT), University of California, Los Angeles, Los Angeles, CA 90095, USA

California NanoSystems Institute (CNSI), University of California, Los Angeles, Los Angeles, CA 90095, USA

Dayong Chen,
Department of Materials Science and Engineering, University of California, Los Angeles, CA 90095, USA

Na He,
Department of Chemistry and Biochemistry, University of California, Los Angeles, CA 90095, USA

Pia Ramos,
Department of Civil and Environmental Engineering, University of California, Los Angeles, CA 90095, USA

Joel Hayashi,
Center for Minimally Invasive Therapeutics (C-MIT), University of California, Los Angeles, Los Angeles, CA 90095, USA

kaner@chem.ucla.edu, sheikhi@psu.edu.

Conflict of Interest

The authors declare the following competing financial interest(s): B.M., E.R., and R.B.K. have an equity interest in Silq Technologies, Corp., which has licensed technology from UCLA on this work.

Supporting Information

Supporting Information is available from the Wiley Online Library or from the author.

California NanoSystems Institute (CNSI), University of California, Los Angeles, Los Angeles, CA 90095, USA

Paige Curson,
Department of Chemistry and Biochemistry, University of California, Los Angeles, CA 90095, USA

Chueh-Yu Wu,
Department of Bioengineering, University of California, Los Angeles, Los Angeles, CA 90095, USA

Praveen Bandaru,
Center for Minimally Invasive Therapeutics (C-MIT), University of California, Los Angeles, Los Angeles, CA 90095, USA

California NanoSystems Institute (CNSI), University of California, Los Angeles, Los Angeles, CA 90095, USA

Mackenzie Anderson,
Department of Chemistry and Biochemistry, University of California, Los Angeles, CA 90095, USA

Brandon Bui,
Silq Technologies, Corp., Los Angeles, CA 90025, USA

Aref Sayegh,
Department of Urology, Keck School of Medicine of University of Southern California, Los Angeles, CA 90033, USA

Rancho Research Institute, Rancho Los Amigos National Rehabilitation Center, Downey, CA 90242, USA

Shaily Mahendra,
Department of Civil and Environmental Engineering, University of California, Los Angeles, CA 90095, USA

Dino Di Carlo,
Department of Bioengineering, University of California, Los Angeles, Los Angeles, CA 90095, USA

Evgeniy Kreydin,
Department of Urology, Keck School of Medicine of University of Southern California, Los Angeles, CA 90033, USA

Rancho Research Institute, Rancho Los Amigos National Rehabilitation Center, Downey, CA 90242, USA

Ali Khademhosseini,
Center for Minimally Invasive Therapeutics (C-MIT), University of California, Los Angeles, Los Angeles, CA 90095, USA

California NanoSystems Institute (CNSI), University of California, Los Angeles, Los Angeles, CA 90095, USA

Department of Radiological Sciences, David Geffen School of Medicine, University of California – Los Angeles, Los Angeles, CA 90095, USA

Department of Chemical and Biomolecular Engineering, University of California, Los Angeles, Los Angeles, CA 90095, USA

Department of Bioindustrial Technologies, College of Animal Bioscience and Technology, Konkuk University, Seoul 143-701, Republic of Korea

Amir Sheikhi,
Department of Chemical Engineering, The Pennsylvania State University, University Park, PA 16802, USA

Department of Biomedical Engineering, The Pennsylvania State University, University Park, PA 16802, USA

Richard B. Kaner
Department of Chemistry and Biochemistry, University of California, Los Angeles, CA 90095, USA

Silq Technologies, Corp., Los Angeles, CA 90025, USA

California NanoSystems Institute (CNSI), University of California, Los Angeles, Los Angeles, CA 90095, USA

Department of Materials Science and Engineering, University of California, Los Angeles, CA 90095, USA

Abstract

Unlike growth on tissue, microbes can grow freely on implantable devices with minimal immune system intervention and often form resilient biofilms that continuously pump out pathogenic cells. The efficacy of antibiotics used to treat infection is declining due to increased rates of pathogenic resistance. A simple, one-step zwitterionic surface modification is developed to significantly reduce protein and microbial adhesion to synthetic materials and demonstrate the successful modification of several clinically relevant materials, including recalcitrant materials such as elastomeric polydimethylsiloxane. The treated surfaces exhibit robust adhesion resistance against proteins and microorganisms in both static and flow conditions. Furthermore, the surface treatment prevents the adhesion of mammalian fibroblast cells while displaying no cytotoxicity. To demonstrate the clinical efficacy of the novel technology in the real-world, a surface-treated, commercial silicone foley catheter is developed that is cleared for use by the U.S. Food and Drug Administration (K192034). 16 long-term catheterized patients received surface-treated catheters and completed a Patient Global Impression of Improvement (PGI-I) questionnaire. 10 out of 16 patients described their urinary tract condition post implantation as “much better” or “very much better” and 72% ($n = 13$) of patients desire to continue using the surface-treated catheter over conventional latex or silicone catheters.

Graphical Abstract

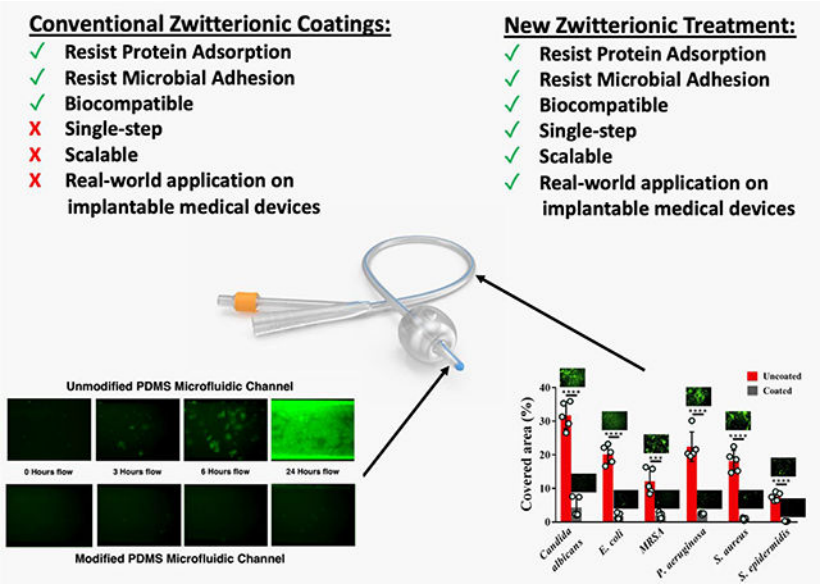

A simple process has been developed to treat the surfaces of implantable medical devices with zwitterionic materials to reduce hospital acquired infection and complications. The process meets the regulatory and scalability requirements to treat real-world devices. Long-term catheterized patients who replaced conventional catheters with surface-treated catheters report improved urinary tract condition and quality of life.

Keywords

antibiofouling; antimicrobial stewardship; cross-linkable coating modification; protein repellant; universal surface treatment; zwitterionic surfaces

1. Introduction

According to a national survey performed in 2007, about 1.7 million hospital-acquired infections (HAIs) are reported annually, accounting for more than 99 000 deaths and ~$30 billion in direct medical costs.[1] Despite the reduction of HAIs in recent years through improved antiseptic techniques, surgical procedures, and diagnosis, HAI declines are slowing down indicating the need for new preventive methods.[2] It is estimated that 60–70% of HAIs are associated with the use of implantable medical devices. These infections occur due to the colonization of bacteria on the device surfaces and most, if not all, devices are affected.[3]

It is estimated that half of all HAIs are attributed to the growth of biofilms.[4] Biofilms form when replicating bacterial cells secrete extracellular polymeric substances that contain an insoluble mixture of proteins and polysaccharides.[5] This 3D gelatinous matrix protects the pathogenic cells from the host defense mechanisms and reduces the diffusion rate of antimicrobials through the matrix, rendering the cells within the biofilm significantly more resistant to antibiotics than in their planktonic state.[6] Furthermore, biofilms are linked to recurring infections, and already-formed biofilms are extremely difficult to resolve.[7] As

medical device surfaces are a nidus for biofilm growth, significant research has focused on the prevention of biofilm growth to reduce device associated HAIs.[8–10]

The biofilm formation cascade is initiated by planktonic bacterial cell adhesion to a surface. Without initial attachment, the biofilm formation is prevented or reduced. Early research on biofilm growth demonstrated that weak van der Waals forces and hydrophobic interactions enable the first colonizers to reversibly adhere to surfaces.[11,12] Using self-assembled monolayers, Whitesides et al. surveyed several functional groups to determine surface functionalities that promote or hinder the nonspecific adsorption of proteins.[13,14] The functional groups that exhibited the lowest adhesion were electrostatically neutral, hydrophilic moieties that contained hydrogen bond donating groups.[13] From these design rules, many material coatings have been developed and shown to reduce adhesion of proteins and microorganisms. However, these coatings are substrate dependent, require pretreatment steps, and/or require exotic reaction conditions that do not enable the surfaces to be permanently modified.[15–21] For these reasons, commercial use of antifouling coatings in medical devices are uncommon. Current commercial coatings often rely on the elution of antibiotics from a polymer matrix that are costly and only partially effective,[10] and further promote antimicrobial resistance.

Here, we describe a permanent antifouling surface treatment that resists protein and bacterial adhesion utilizing a simple, scalable photo-activated treatment. Our criteria for the development of the surface treatment were as follows: 1) the treatment chemistry must be able to permanently bind to clinically relevant plastics and rubbers; 2) the surface treatment must be nontoxic; 3) the treatment must be applied rapidly under ambient conditions to maintain the scale of medical device manufacturing; and 4) the treatment must not incorporate antibiotics to maintain global antimicrobial stewardship efforts. The zwitterionic polymer polysulfobetaine (PSB) was selected as the antifouling component of the surface modification to benefit from its biocompatibility, ultralow-fouling properties, and oxidative stability. By adsorbing water electrostatically, PSB coatings form a thin hydration barrier that prevents organic materials from adhering to surfaces.[22] Commonly used approaches to attach PSB coatings to surfaces, such as radical-initiated graft polymerizations of PSB-methacrylate necessitate the use of oxygen-free conditions,[23] preconditioning steps,[24] or long reaction times[25] that do not meet scalability requirements. To circumvent the use of air-free graft polymerizations, we employ perfluorophenylazide (PFPA) chemistry as a molecular anchor to link the PSB coatings onto the surfaces of polymeric materials under ambient conditions. When triggered with UV-light, PFPA moieties generate a highly reactive nitrene that forms covalent bonds with materials containing amines, C=C double bonds, and C–H bonds.[26,27] With this method, PSB is rapidly coated onto a broad range of substrates using UV light under ambient conditions with no preconditioning steps. Thus, many different medical devices may be quickly and conveniently treated on the manufacturing level.

We first demonstrate the effect of the treatment on polydimethylsiloxane (PDMS) as an exemplary, extremely difficultto-modify model for a common elastomer used in implantable medical devices.[28] Commonly known as silicone, PDMS is widely used for its biocompatibility, good chemical stability, ease of fabrication using injection molding

or extrusion, and low cost.[29–31] Many implantable device makers have moved away from classical medical elastomers and plastics such as latex and polyvinyl chloride due to allergens[32] or plasticizers[33] in these materials that leach out and often lead to irritation or complications. PDMS-based devices do not require plasticizers and have been shown to lead to fewer complications than latex and polyurethane-based devices.[34]

Despite its ideal properties, the nonpolar nature of PDMS facilitates the adhesion of organic materials. Bacteria, platelets, proteins, and other biomolecules bind strongly to the hydrophobic surfaces of PDMS elastomers, leading to the colonization and proliferation of biofilms.[22] When common hydrophilic surface treatments are performed on PDMS, such as plasma oxidation,[35] UV-ozone,[36] or corona discharge,[37] the effects are short-term due to rapid hydrophobic recovery. The highly mobile chains of PDMS (glass transition temperature ≈ −120 °C) can reorient themselves to “hide” the surface modified elastomers, when exposed to air, within hours.[38] Other methods seeking long-lasting hydrophilic PDMS surfaces typically require preconditioning steps with silane[39–41] chemistry or radical polymerization.[39,42] These steps must be performed in closed containers, and/or under the protection of inert gas. Due to the high solubility of oxygen relative to nitrogen in PDMS,[43] additional steps and time are required to remove the oxygen from PDMS so that the radical reaction can proceed efficiently. These strict reaction conditions significantly increase the coating costs, limiting the surface modification of PDMS to lab scale demonstrations. With our method, for the first time, PDMS substrates can be rapidly modified under ambient conditions, without pretreatment. We then demonstrate the surface treatment’s exceptional antibiofouling efficacy by challenging it against protein, mammalian cells, bacteria, and fungus in vitro. To demonstrate the clinical performance of the treatment technology, silicone indwelling catheters were treated, cleared by the U.S. Food and Drug Administration (K192034), and implanted in vivo in spinal cord injury patients at a National Rehabilitation Center. Catheters are one of the most common medical devices used in hospitals and thus greatly contribute to device-related complications, such as encrustation, occlusion, and Catheter-associated urinary tract infection.[44,45]

2. Results and Discussion

A PSB polymer combined with PFPA (PFPA-PSB), provided by Silq Technologies, Corp., was added to water at different concentrations to make a pretreatment solution. To fabricate PDMS substrates, liquid Sylgard 184 was cast in Petri dishes, cured, and modified with the PFPA-PSB pretreatment solution upon exposure to 254 nm UV light. Upon UV exposure, the nitrene group simultaneously binds to the PDMS surface and causes the PFPA-PSB polymer to undergo cross-linking. The chemical structure of PSB and PDMS are shown in Figure 1a. The X-ray photoelectron spectroscopy (XPS) analysis of a treated PDMS substrate (Figure 1b) shows the presence of the elements S and N in the coated PDMS (shown with blue arrows in Figure 1b), an indication of the successful binding of the photo-cross-linkable polymer on the organic substrate. The ability of the nitrene to undergo C–H insertion and form azo compounds causes the polymer to simultaneously bind to the substrate and cross-link (Figure 1c). Also, we hypothesized that the cross-linked network of PFPA-PSB would impede the hydrophobic recovery of the PDMS substrate. To determine this, the water contact angle on the PSB-coated PDMS was compared with

that of oxygen plasma-treated substrates every 2 days over a 10-day period. Figure 1d presents the time evolution of contact angle on these two substrates. The O_2 plasma-treated PDMS exhibited an initial contact angle ≈10°, which increased to >40° after 2 days. The contact angle of plasma-treated PDMS continued to increase over time until it reached ≈90° after 10 days, that is, the contact angle of untreated PDMS. PSB-coated PDMS, however, maintained a contact angle ≈15° after 2 days, which was significantly lower than the plasma treated substrate. After 10 days, the PSB-coated PDMS retained a contact angle of <25°, demonstrating its ability to prevent hydrophobic recovery. Similarly, a variety of clinically relevant polymeric substrates were coated with PFPA-PSB and their water contact angles were studied. Figure 1e presents the water contact angles on PSB-coated PDMS, nylon 66, polystyrene, polyvinyl chloride, and polyethylene, showing that all the substrates had been successfully modified and acquired a hydrophilic surface compared with the unmodified ones, which all had apparent contact angles of >60°.

Our surface modification with the zwitterionic material provides a platform to impart antibiofouling properties to a wide range of substrates. We focused on PDMS for its popularity of use in biomedical devices[46] and the ability of PFPA-PSB treatment to impede the hydrophobic recovery of PDMS for long-term applications. Protein adsorption on substrates plays an important role in initiating the attachment of biological species. Proteins such as fibrinogen are typically coated on substrates to convert them into cell adhesive materials for cell culture applications.[47,48]

To investigate the PSB modification's ability in preventing protein adhesion to the inner lumen of implantable devices under flow conditions, microfluidic channels were fabricated. Microfluidics provides a powerful platform to study the effects of protein adhesion and cellular growth under both static and flow conditions. PDMS is the most popular material used in microfluidic devices for its ease of fabrication and transparency.[49,50] However, the hydrophobic microfluidic channel walls facilitate rapid binding of proteins and organic materials, diminishing experimental accuracy and impairing data collection.[51] Because PDMS is transparent to UV light, the channel walls can be readily modified using our system. Fluorescent fibrinogen was selected as the analyte protein due to its availability and role in bacterial adhesion and blood clotting. Fibrinogen deposition, in response to tissue damage by catheter implantation, is the critical pathogenic event in the colonization of *Enterococcus Faecalis* and other bacteria, which is initiated by pili containing fibrinogen-binding adhesins attachment to deposited fibrinogen on catheters.[52–54] Furthermore, catheter-related thrombosis is a frequent problem in central venous catheters, in part due to the adherence of fibrinogen to the catheter tip,[55] causing fibrin sheath formation[56] that leads to occlusion.[57]

For both the flow and static experiments, solutions of 10 and 100 μg mL^{-1} fluorescent fibrinogen in deionized (DI) water were prepared and passed through 1 mm microfluidic channels, respectively. The experiments were initiated by pumping the fibrinogen solution through the channel via a syringe pump at a rate of 10 μL min^{-1} and monitoring the channel under a microscope (Figure 2a). Images were recorded 5 s after the channel was filled with the solution (t = 5 s), then recorded at 5-min intervals for 15 min with an exposure time of 1 s. An increase in fluorescence over time as the protein adheres to the

channel walls was attributed to the adhesion and buildup of the fluorescent fibrinogen. Using ImageJ, the mean gray value, representing the average fluorescent intensity for each image, was determined and the percentage increase relative to the initial image (t = 5 s) was calculated (Figure 2b). The fluorescent intensity in bare PDMS channels increased by ≈138%, 217%, and 280% after 5, 10, and 15 min, respectively. For the PSB-coated PDMS channel, the fluorescent intensities increased ≈21%, 27%, and 32% for the 5, 10, and 15-min images, respectively, which mainly corresponds to the background fluorescent flow. The static adhesion experiment demonstrates the ability of the PSB modification to reduce the interactions between the surfaces and proteins. A bare and a coated channel were filled with a 10 μg mL^{-1} solution of fluorescent fibrinogen in DI water and maintained for 30 min before DI water was flushed through the channel to remove nonadherent fibrinogen, followed by imaging at an exposure of 500 ms. For the unmodified channel, the protein was well adhered and was not removed during the DI water rinse. For the modified channel, the DI rinse completely removed the weakly bound fibrinogen from the walls of the channel. The reduction of protein adsorption is attributed to the formation of a strongly bound hydration layer at the PSB-medium interface, significantly decreasing the electrostatic and hydrophobic interactions between the protein and the PDMS substrate.[23,58,59] When uncoated and PFPA-PSB coated silicone tubes were placed in a closed blood lube system containing fresh circulating ovine blood, large thrombi formed on the unmodified tubes. The modified tubes prevented large thrombi from forming on the surface and exhibited antithrombogenic properties, as shown in the Figure S1, Supporting Information.

Figure 3 presents the behavior of NIH/3T3 fibroblast cells seeded on PSB-modified cell culture well plates compared with uncoated wells. Bright field images of the uncoated wells (Figure 3a) demonstrate that the cells tend to adhere and spread on the substrate within a few hours, whereas the PSB-modified wells completely inhibit the cell adhesion, resulting in cell detachment and aggregation in the medium. The insets of the images display high magnification views of the nonadhered cells for better visualization of their morphology. We have also stained the cells using a live/dead assay after 24 h of culture to assess their viability. Fibroblast cells cultured on uncoated well plates and PSB-modified well plates were fixed using the live/dead staining, as shown in Figure 3b. While the uncoated wells permit the attachment and survival of almost 100% of the cells, the PSB-modified substrates prevented cell attachment, resulting in cell death. The detached cells were washed off during the staining process. The negative control included the cell culture in dimethylsulfoxide (DMSO), resulting in complete cell death. Figure 3c presents the shape factor of the cells 24 h post seeding, measured from $4\pi A/P^2$, where A is the cell surface area and P is the perimeter obtained from analyzing at least 20 cells per sample after live/dead staining. When the shape factor is ≈1, the cells adopt a spherical shape, and the elongated cells render a shape factor <<1 (0 represents a straight line).[60] The shape factor of cells cultured on uncoated well plates is ≈0.2, attributed to an elongated morphology as a result of cell spreading. At PFPA-PSB concentration of >2 mg mL^{-1}, the shape factor of cells is >0.85, indicating a near-spherical morphology. Furthermore, the percentage of cells adhered to the substrate normalized with the seeded cells is presented in Figure 3d. The top panels reveal cell proliferation on the uncoated PDMS substrate after 24 h (reflected in the

values of >100%), while the PSB-coated PDMS substrates do not support the adhesion and proliferation of cells.

To demonstrate the adhesion resistance of pathogenic cells, bacterial and fungal cells were incubated directly on bare and PSB-coated PDMS substrates, stained with Syto 9 fluorescent nucleic acid dye, and analyzed with fluorescent microscopy. Figure 4a displays images of the substrates using fluorescent microscopy (inset) and quantitative analysis results from microbial adhesion after 24–48 h of incubation on PSB-modified and unmodified surfaces. The PSB-modified surfaces significantly decreased the bacterial and fungal adhesion as well as the biofilm formation compared with the unmodified surfaces across all tested microorganisms. The surface treatment reduced the biofouling by inhibiting the attractive interactions of microorganisms with anchoring proteins responsible for bioadhesion,[56] impairing bacterial adhesion and/or biofilm forming cascades. Similar results were obtained when a fluorescent *Escherichia coli* (*E. coli*) solution was flowed through the uncoated and coated microfluidic channels for 24 h, as can be seen in Figure 4b. In the bare PDMS channel, *E. coli* adhesion to the channel walls was observed after 3 h and continued to increase and form a thick film after 24 h. In contrast, the bacterial adhesion to the PSB-coated channels was scarce even after 24 h of flow. Figure 4c presents the dynamics of increase in intensity based on the quantification of fluorescent images in Figure 4b. While the bacterial flow rendered the uncoated channels green, yielding more than 160% increase in intensity in only 24 h, the coated channels remained protected against the bacterial adhesion and did not show a significant increase in the fluorescent intensity.

The cytotoxicity of PFPA-PSB was investigated by dissolving PFPA-PSB powder in the fibroblast cell culture media and monitoring the behavior of cultured monolayer cells for 72 h, as shown schematically in Figure 5a. The metabolic activity of the cells is quantified based on the reduction of MTT (3-(4,5-dimethylthiazol-2-yl)-2,5-diphenyltetrazolium bromide) by viable, metabolically active cells, which is detected by the fluorescent intensity alteration due to the formation of intracellular purple formazan. The fluorescent intensity was normalized with that of cells cultured in PSB-free media after 24, 48, and 72 h. After being exposed to concentrations of up to 1600 μg mL^{-1} of PFPA-PSB for 72 h, no significant decreases in the metabolic activity of cells were detected, that is, PSB did not compromise the cell viability. When the cells were stained with a live/dead assay, presented in Figure 5b, the behavior of cells exposed to PFPA-PSB solution was identical to PSB-free cells, which all exhibited ≈100% viability. To determine the cytotoxicity of the PSB modification (cross-linked PSB), untreated and treated PDMS discs were incubated directly in the cell culture media of a monolayer fibroblast cell culture, as shown schematically in Figure 5c. The metabolic activity of cells incubated with the PDMS substrates or PSB-coated PDMS substrates in the media was also identical to the control (cells not exposed to any PDMS substrate), indicating the excellent biocompatibility of the treatment. After the live/dead staining (Figure 5d) of fibroblast cells incubated with the coated PDMS discs, we observed no difference in toxicity between the uncoated and coated PDMS surfaces, further confirming the safety of the treatment material to the cells. Accordingly, PSB provides a safe platform for the surface modification of polymeric materials used in medical devices that are in direct contact with tissues and organs.

Figure 5e presents the hemolysis of red blood cells (RBCs) in the presence of uncross-linked PFPA-PSB, demonstrated by the optical images of varying concentrations of PFPA-PSB in heparinized human whole blood after centrifuging. The red color indicates the release of hemoglobin in the media due to the damaged RBCs. Figure 5f presents the hemolysis percentage of RBCs in the presence of PFPA-PSB compared with the positive control (PC, Triton X-100) and negative control (NC, polyethylene glycol [PEG]). The hemolysis percentage induced by the uncross-linked PFPA-PSB was not significantly different from the negative control when the polymer concentration was <2 mg mL^{-1}, which increased to only about 6% at 10 mg mL^{-1} of PFPA-PSB. The ASTM E2524-08 (2013) guideline indicates that the permissible level for hemolysis is ≤5%. According to independent lines of evidence, uncross-linked PFPA-PSB (<10 mg mL^{-1}) is nontoxic for the cells, which provides a suitable material for modifying medical devices that are in contact with cells.

To assess the clinical impact of the surface treatment, 18 patients, 9 males and 9 females, were recruited. Four patients managed their bladder with a urethral catheter, while the remainder managed their bladder with a suprapubic catheter. All patients suffered from voiding dysfunction due to neurogenic bladder as a result of spinal cord injury (n = 15), multiple sclerosis (n = 1) or muscular dystrophy (n = 2). 16 patients completed the PGI-I questionnaire prior to their return visit for catheter exchange. 10 out of 16 of the patients described their urinary tract condition post implantation as “very much better” (n = 6) or “much better” (n = 4), and 5 of the patients described their urinary tract condition as a “little better” (n = 1) or no change (n = 4). The majority of patients (76%, n = 13) elected to continue with a surface-treated catheter, while the remainder elected to return to the catheter that was used originally (n = 4). Among all patient comments, decrease in obstruction episodes and the need to irrigate to keep the catheter open was noted by 52% (n = 9), “less bacteria/less infection” by 24% (n = 4), “less pain” by 12% (n = 2), and “less odor” by 6% (n = 1).

In this contribution, we have developed a simple technology to transform the surfaces of materials commonly used in implantable medical devices to reduce infections and complications. We combined the high reactivity of PFPA chemistry and the antibiofouling properties of zwitterionic chemistry to successfully coat several clinically relevant polymers under ambient conditions. PDMS, one of the most common elastomers used in medicine and arguably the most difficult to modify, was readily modified with our process. The coated PDMS exhibits nominal hydrophobic recovery, exhibiting long-term antibiofouling performance. To investigate the surface treatment’s efficacy under flow conditions, the inner walls of microfluidic channels were modified and displayed exceptional antibiofouling properties under static and dynamic conditions, which otherwise significantly underwent biofouling. To demonstrate the clinical potency of the technology in patients, treated-silicone foley catheters were used to replace conventional catheters in neurogenic bladder patients. 9 of the patients reported a decrease in obstruction episodes, 10 of the patients reported “very much better” or “much better” bladder condition with use of the treated-catheter, and 13 of 16 patients desired to continue using the treated-catheter after the study period was over. The technology can be easily applied as a universal surface treatment for a wide variety of medical devices, and will be extended to other applications where biodeterioration and biofouling must be controlled.

3. Experimental Section

Materials:

PDMS base and the curing agent (SYLGARD 184 Elastomer Kit, Dow Corning, MI, USA) were used to make the PDMS substrates and channels. The PSB polymer containing PFPA moieties was provided by Silq Technologies, Corp., CA, USA. Nylon 6/6, polystyrene, polyvinyl chloride, and polyethylene slabs were all purchased from McMaster-Carr, CA, USA. Milli-Q water (electrical resistivity ≈18.2 MΩ cm at 25 °C) was provided by Millipore Corporation. NIH/3T3 fibroblast cells were from the American Type Culture Collection (ATCC, VA, USA). Dulbecco's phosphate-buffered saline (DPBS) solution and Dulbecco's modified Eagle medium (DMEM) was from Gibco by Thermo Fisher Scientific, PA, USA. Fetal bovine serum (FBS, Benchmark by Gemini Bio-Products) and penicillin/streptomycin (P/S, Sigma-Aldrich) were used to supplement DMEM. Trypsin-ethylenediaminetetraacetic acid (EDTA) (0.5%, 10×), LIVE/DEAD viability/cytotoxicity kit, and MTT ((3-(4,5-dimethylthiazol-2-yl)-2,5-diphenyltetrazolium bromide) cell viability reagent were from Invitrogen by Thermo Fisher Scientific (OR, USA). Cell culture flasks (75 cm^2, Corning, NY, USA) and polystyrene 96- or 48-well tissue culture-treated plates (Falcon, NC, USA) were used to culture cells. The light source was Spectroline UV lamp model ENF-260C (NY, USA). Microbial species were purchased from ATCC. Luria-Bertani (LB), nutrient broth, trypticase soy broth (TSB), and yeast mold broth were obtained from Fisher Scientific. SYTO 9 live/dead Baclight Bacterial Viability Kit L13152 was from Molecular Probes. Fibrinogen from human plasma, Alexa Fluor 546 conjugate was provided by Thermo Fisher Scientific, Inc. Drabkin's solution, pure human hemoglobin, PEG, and Triton X-100 were provided by Sigma-Aldrich (MO, USA).

Treating Substrates with PSB:

PDMS substrates were prepared by mixing a 10:1 ratio of elastomer:curing agent (Syglard 184), followed by curing at 80 °C for 1 h. The PDMS sheets were cut with a laser cutter into 3 mm diameter disks. A PSB pretreatment solution (30 μL) with a concentration of ≈2, 5, or 10 mg mL^{-1} was placed and spread out on the surface of each disk, followed by cross-linking on the discs by exposure to 254 nm UV light for 10 min under sterile conditions, rinsing with Milli-Q water, and drying with air.

Contact Angle Visualization and Measurement:

Water contact angle on various substrates, such as PDMS, nylon 66, polystyrene, polyvinyl chloride, and polyethylene was visualized by placing ≈17 μL of Milli-Q water on the flat substrates at room temperature followed by imaging them. The images were analyzed using the FTA32 version 2.1 software to measure the contact angles. To study the recovery of water contact angles on PDMS substrates, the substrates were divided into two groups: 1) uncoated PDMS sheets, which were treated using O_2 plasma (Plasma Etch PE25-JW Plasma Cleaner, NV, US) for 1 min, followed by measuring the water contact angle after 1, 2, 4, 7, and 10 days, and 2) PDMS sheets that were coated with PSB, and the contact angle was similarly measured over time. New samples were measured each time for each corresponding time period.

X-Ray Photoelectron Spectroscopy:

A Kratos AXIS Ultra DLD with a monochromatic Al Kα X-ray source operated at 10 mA and 15 kV was used to perform XPS. The authors collected individual high-resolution spectra and survey spectra using 20 and 160 eV pass energies, respectively. Data processing was carried out using CasaXPS 2.3 software. The spectra binding energies were calibrated by realizing the hydrocarbon peak in the C1s high-resolution spectra at 284.6 eV.

Microbial Culture:

All microbes used in this work were purchased from American Type Culture Collection (ATCC, Manassas, VA): *E. coli* (ATCC-15597), *Staphylococcus epidermidis* (ATCC-14990), *Staphylococcus aureus Rosenbach* (ATCC-12600), *Staphylococcus aureus MRSA* (ATCC-BAA1754), *Pseudomonas aeruginosa* PAO1 (ATCC-10145), and *Candida albicans* (ATCC-18804). All strains were incubated at 37 °C at 150 rpm until a midexponential phase was acquired to harvest the cells by centrifugation at 3800 × *g* for 8 min. *E. coli* was grown on a Luria-Bertani (LB) broth; *S. epidermidis, P. aeruginosa*, and *S. aureus Rosenbach* were grown on nutrient broth; *S. aureus* (MRSA) was grown on a TSB; and *C. albicans* was grown on a yeast mold broth. These initial cultures were then adjusted to an optical density of 1 at 600 nm and had an initial total cell number ranging from 1×10^7 cells per mL to 1×10^8 cells per mL, as confirmed by plate counting.

Microfluidic Channel Modification and Protein Adsorption Evaluation:

PDMS microfluidic channels were fabricated using conventional soft lithography, and fluorescent fibrinogen (Fibrinogen Alexa Flour 546) was utilized for static and flow experiments to evaluate the repelling effect of surface treatment against protein adsorption in microfluidic channels. Simple straight PDMS channels (150 μm tall and 600 μm wide) were replicated from a mold of SU-8 photoresist (MicroChem, Corp.) on a 4-inch wafer. The mold was fabricated by standard photolithography, involving the spin-coating of a photoresist layer on the wafer, illuminating UV through a mask with the designed pattern of the channel, and developing the pattern with the SU-8 developer. The PDMS precursor (Sylgard 184) and cross-linker were mixed in a 10:1 ratio, poured onto the mold, degassed in a desiccator, and incubated in an oven at 60 °C overnight. The cross-linked PDMS was cut and peeled out of the mold, punched with two holes for inlet and outlet, and covalently bonded onto a glass slide after plasma treatment. The surface-treated channels were filled with a PSB solution via syringe and irradiated with 254 nm UV light (Spectroline UV lamp model ENF-260C) for 10 min. The handheld UV lamp was held 2 inches above the channel with the PDMS side facing up (glass slide facing down). The treated channels were then rinsed by flushing the channels with 3 mL of DI water three times to remove any unbound agglomerates. The static experiment was conducted by incubating fibrinogen inside the sealed PDMS channel for 30 min. The channel was rinsed with DI water and then imaged using a fluorescent microscope. For the flow experiment, fibrinogen was pumped through the PDMS channel by a syringe pump (PHD 2000, Harvard Apparatus, Inc.) with a flow rate of ≈10 μL min^{-1}. The channel was taped onto the stage of the microscope for imaging every 5 min.

Microbial Adhesion:

Petri dishes (diameter ≈55 mm) were filled with ≈5 mL of a 10:1 elastomer to curing agent (Sylgard 184) and allowed to cure at room temperature for at least 48 h. The fabricated PDMS discs were 3 mm thick and filled the bottom of circular 2″ inner diameter Petri dishes. Modified plates were coated with a solution containing PSB and irradiated with 254 nm UV light as explained previously. Each modified and unmodified PDMS-lined dish was inoculated with 4 mL of bacterial or fungal suspensions and incubated for 24–72 h (shaken at 25 rpm) at 35 °C. The Petri dishes were gently rinsed with sterile, deionized water using a Pasteur pipette, and covered in 4 mL of a dye solution (SYTO 9 live/dead Baclight Bacterial Viability Kit L13152) for 15 min. The SYTO 9 solution was prepared by dissolving the contents of component A of the kit in 30 mL of sterile, deionized water. After the staining was complete, the Petri dishes were gently rinsed with deionized water and imaged using a 4× CCD camera (Axiocam MRm System) attached to a Zeiss Axioskop 2 microscope with a 10× objective, 40× objective, a fluorescent lamp, and a blue excitation filter. During observation, five images were taken at an excitation range of 450–490 nm. The identification of attached microorganisms in all fluorescent images was determined using ImageJ software. The dynamic bacterial adhesion experiments were conducted by flowing a fluorescent *E. coli* solution (10^8 cells/mL) through the uncoated and PSB-coated microfluidic PDMS channels for 24 h.

Cell Culture:

NIH/3T3 fibroblast cells were cultured in cell culture flasks containing DMEM with 10% FBS and 1% P/S and passaged twice a week. For this purpose, a standard cell culture incubator (Thermo Fisher Scientific, PA, USA) was used to provide 5% CO_2 atmosphere and temperature of 37 °C. To conduct cell studies, 0.5% trypsin-EDTA was used to trypsinize fibroblast cells and they were counted using a hemocytometer, followed by seeding them on coated or uncoated substrates.

Cell Adhesion:

Trypsinized fibroblasts cells were seeded on PSB-coated 96-well plates by placing 100 μL of the cell suspension (cell density ≈1×10^5 in 1 mL media) on the treated well plates, followed by culturing for 24 h. Uncoated well plates were used as a control.

Cytotoxicity Evaluation:

To assess the cytotoxicity of uncross-linked PSB, trypsinized fibroblasts cells were seeded on 96-well plates by placing 100 μL of the cell suspension (cell density ≈1×10^5 in 1 mL media), cultured for 24 h, and followed by adding a desired amount of uncross-linked PSB to the media and further culturing for 72 h. Furthermore, the cytotoxicity of cross-linked PSB was evaluated by seeding 500 μL of cell suspension (cell density ≈2×10^5 in 1 mL media) in 24-well plates, cultured for 24 h, followed by placing PSB-coated PDMS discs (diameter ≈ 6 mm, height ≈ 3 mm) in the medium and further culturing for 72 h.

Metabolic Activity Assessment:

MTT ((3-(4,5-dimethylthiazol-2-yl)-2,5-diphenyltetrazolium bromide) (Thermo Fisher Scientific) stain solutions were prepared at a concentration of ≈5 mg mL^{-1} in DPBS. Cell culture media were removed from the well plates, followed by one-time rinsing with DPBS. The wells were then loaded with fresh media including the MTT solution at a ratio of 9:1. The well plates were wrapped with aluminum foil and incubated for 4 h at 37 °C and 5% CO_2. After 4 h, the wells were aspirated with a pipette, and 200 and 500 μL of DMSO was added to the 24- and 96-well plates, respectively. The well plates were wrapped with aluminum foil again and left on a rotator for 30 min after which absorbance was recorded at 570 nm using a microplate reader (Synergy HTX multimode reader, BioTek, VT, USA).

Live/Dead Assay:

To assess the cell viability, a live/dead fluorescence assay was used. The staining solution was prepared by adding ethidium homodimer-1 (20 μL) and calcein AM (5 μL) to DPBS (10 mL). To perform the assay, the cells were incubated with 1 mL of the staining solution for ≈20 min and imaged using a fluorescent microscope (Axio Observer 5, Zeiss, Germany) at excitation/emission wavelengths ≈494/515 nm for calcein and 528/617 nm for ethidium homodimer-1.

Hemolytic Properties Characterization:

Hemolysis assay was performed using ASTM standard E2524-08 (2013) method to determine the concentration of hemoglobin released in plasma (i.e., plasma-free hemoglobin) when blood was exposed to the polymers. The principle of the assay was based on oxidization of methemoglobin by cyanide (Drabkin's solution) to form cyanmethemoglobin, which was quantified by a colorimetric method using a spectrophotometer at 540 nm. Briefly, total hemoglobin concentration in heparinized human whole blood (provided by volunteers) was measured based on a standard curve obtained from pure human hemoglobin at concentrations ranging from 0.025 to 0.80 mg mL^{-1}. The blood was further diluted in DPBS to a total hemoglobin concentration of 10 ± 2 mg mL^{-1}. All tests were performed in triplicate using the blood pool obtained from three different donors. Polymer samples (100 μL in DPBS) with varying final concentrations were added to 700 μL of DPBS in centrifuge tubes and gently mixed with 100 μL of diluted whole blood. The samples were then incubated at 37 °C for 3 h ± 15 min, followed by centrifugation for 15 min at 800 × *g* at room temperature. The supernatant (100 μL) was then mixed with an equal volume of Drabkin reagent in 96-well plates and allowed to react in dark for 15 min at ambient temperature. The absorbance of samples was obtained at 540 nm against the reagent blank using a microplate reader (BioTek UV/Vis Synergy 2, VT, USA) and was subtracted from the background absorbance (i.e., blood-free samples) at the same wavelength. Finally, the concentration of hemoglobin in each sample was determined from the standard curve by taking the dilution factor (18) of the samples and controls into account. The percent hemolysis was then calculated by dividing the hemoglobin concentration of samples by the total blood hemoglobin (≈10 mg mL^{-1}) and reported in percentage. To monitor the assay performance, 4.4% PEG and 1% Triton X-100 were used as negative and positive controls, respectively.

Statistical Analysis:

The data were reported as mean values ± standard deviation of at least triplicate experiments. The one-way analysis of variance and Tukey's multiple comparisons were used, and statistically significant differences were identified for p-values lower than 0.05 (*$p < 0.05$), 0.01 (**$p < 0.01$), 0.001 (***$p < 0.001$), and 0.0001 (****$p < 0.0001$).

Assembly of Surface-Treated Catheters for Patients:

16 French, 5 mL balloon silicone foley catheters were treated under current good manufacturing practice on a custom surface-treatment apparatus inside of a clean room. The treated-catheters were packaged in Tyvek pouches (Amcor, Commerce, CA) and sterilized with ethylene oxide (STERIS, Temecula, CA). The treated-catheters met or exceeded the recommended guidelines by the FDA for the biological evaluation of medical devices for Class 2 devices (ISO 10993-1).

The clinical portion of the study was approved by the Institutional Review Board of Rancho Research Institute (#475), the research arm of Rancho Los Amigos National Rehabilitation Center. Patients with inability to void volitionally, who managed their lower urinary tract with an indwelling catheter (urethral or suprapubic) for at least 1 year were recruited. Patients who used latex and silicone catheters were permitted in the study. The surface-treated catheter was inserted using standard technique via the urethra or pre-existing suprapubic tract. The patients returned at their designated interval (2–4 weeks) or for an unscheduled visit if they experienced any problems with the catheter. At the time of their follow up visit, the patients chose whether to continue with the surface-treated catheter or to return to their original catheter. They were asked to complete the Patient Global Impression of Improvement (PGI-I) scale and their feedback on the PSB surface-treated catheter was recorded. The PGI-I was a questionnaire scale (ranging from [1] = Very Much Better to [7] = Very Much Worse) that was widely used in clinical practice and research to assess patient impression of an intervention.[61,62] PGI-I scores were tabulated, and patient comments were abstracted and tabulated (Table S1, Supporting Information).

Supplementary Material

Refer to Web version on PubMed Central for supplementary material.

Acknowledgements

B.M., A.P., and E.R. contributed equally to this work. The authors thank the following for financial support: the Canadian Institutes of Health Research (CIHR) through a postdoctoral fellowship (A.S. - Sheikhi), the National Institutes of Health (1R01EB024403, HL137193, 1R01GM126831) (A.K.), the National Science Foundation CBET 1337065 and CERC-WET (R.B.K.), Silq Technologies, Corp., (R.B.K.), National Science Foundation CAREER 1255021 (S.M.), and the UCLA Sustainability Grand Challenge (S.M. and R.B.K.).

Data Availability Statement

The data that support the findings of this study are available from the corresponding author upon reasonable request.

References

[1]. Klevens RM, Edwards JR, Richards CL Jr., Horan TC, Gaynes RP, Pollock DA, Cardo DM, Public Health Rep. 2007, 122, 160. [PubMed: 17357358]

[2]. Centers for Disease Control and Prevention, 2006–2016, 2017.

[3]. Bryers JD, Biotechnol. Bioeng 2008, 100, 1. [PubMed: 18366134]

[4]. Herman-Bausier P, Dufrêne YF, Science 2018, 359, 1464. [PubMed: 29599229]

[5]. Flemming H, Wingender J, Szewzyk U, Steinberg P, Rice SA, Kjelleberg S, Nat. Rev. Microbiol 2016, 14, 563. [PubMed: 27510863]

[6]. Lebeaux D, Ghigo J, Beloin C, Microbiol. Mol. Biol. Rev 2014, 78, 510. [PubMed: 25184564]

[7]. Römling U, Balsalobre C, J. Intern. Med 2012, 272, 541. [PubMed: 23025745]

[8]. Percival SL, Suleman L, Vuotto C, Donelli G, J. Med. Microbiol 2015, 64, 323. [PubMed: 25670813]

[9]. Rodrigues LR, Bact. Adhes 2011, 715, 351.

[10]. Zhang Z, Wagner VE, Antimicrobial Coatings and Modifications on Medical Devices, Springer, Cambridge, MA, USA 2017.

[11]. Briandet R, Herry J, Bellon-Fontaine M, Colloids Surf., B 2001, 21, 299.

[12]. Takahashi H, Suda T, Tanaka Y, Kimura B, Lett. Appl. Microbiol 2010, 50, 618. [PubMed: 20438621]

[13]. Ostuni E, Chapman RG, Holmlin RE, Takayama S, Whitesides GM, Langmuir 2001, 17, 5605.

[14]. Holmlin RE, Chen X, Chapman RG, Takayama S, Whitesides GM, Langmuir 2001, 17, 2841. [PubMed: 34139796]

[15]. Li G, Cheng G, Xue H, Chen S, Zhang F, Jiang S, Biomaterials 2008, 29, 4592. [PubMed: 18819708]

[16]. Schlenoff JB, Langmuir 2014, 30, 9625. [PubMed: 24754399]

[17]. Jiang S, Cao Z, Adv. Mater 2010, 22, 920. [PubMed: 20217815]

[18]. Smith RS, Zhang Z, Bouchard M, Li J, Lapp HS, Brotske GR, Lucchino DL, Weaver D, Roth LA, Coury A, Biggerstaff J, Sukavaneshvar S, Langer R, Loose C, Sci. Transl. Med 2012, 4, 132.

[19]. a)Mi L, Jiang S, Angew. Chem 2014, 126, 1774;b)Mi L, Jiang S, Angew. Chem., Int. Ed. Engl 2014, 53, 1746. [PubMed: 24446141]

[20]. Cheng G, Zhang Z, Chen S, Bryers JD, Jiang S, Biomaterials 2007, 28, 4192. [PubMed: 17604099]

[21]. Yeh S-L, Wang T-C, Yusa S.-i., Thissen H, Tsai W-B, ACS Omega 2021, 6, 3517. [PubMed: 33585736]

[22]. Zhang H, Chiao M, J. Med. Biol. Eng 2015, 35, 143. [PubMed: 25960703]

[23]. Yang R, Gleason KK, Langmuir 2012, 28, 12266. [PubMed: 22873558]

[24]. Leigh BL, Cheng E, Xu L, Derk A, Hansen MR, Guymon CA, Langmuir 2018, 35, 1100. [PubMed: 29983076]

[25]. Zhou R, Ren PF, Yang HC, Xu ZK, J. Membr. Sci 2014, 466, 18.

[26]. Poe R, Schnapp K, Young MJT, Grayzar J, Platz MS, J. Am. Chem. Soc 1992, 114, 5055.

[27]. Liu L, Yan M, Acc. Chem. Res 2010, 43, 1434. [PubMed: 20690606]

[28]. Lam M, Migonney V, Falentin-Daudre C, Acta Biomater. 2021, 121, 68. [PubMed: 33212233]

[29]. Wolf MP, Salieb-Beugelaar GB, Hunziker P, Prog. Polym. Sci 2018, 83, 97.

[30]. Zhang Y, Liu Y, Ren B, Zhang D, Xie S, Chang Y, Yang J, Wu J, Xu L, Zheng J, J. Phys. D: Appl. Phys 2019, 52, 403001.

[31]. Leng C, Hung H-C, Sun S, Wang D, Li Y, Jiang S, Chen Z, ACS Appl. Mater. Interfaces 2015, 7, 16881. [PubMed: 26159055]

[32]. Brehler R, Kütting B, Arch. Intern. Med 2001, 161, 1057. [PubMed: 11322839]

[33]. Erythropel HC, Maric M, Nicell JA, Leask RL, Yargeau V, Appl. Microbiol. Biotechnol 2014, 98, 9967. [PubMed: 25376446]

[34]. Wildgruber M, Lueg C, Borgmeyer S, Karmov I, Braun U, Kiechle M, Meier R, Koehler M, Ettl J, Berger H, Eur. J. Cancer 2016, 59, 113. [PubMed: 27023050]

[35]. Bodas D, Khan-Malek C, Sens. Actuators, B 2007, 123, 368.

[36]. Oláh A, Hillborg H, Vancso GJ, Appl. Surf. Sci 2005, 239, 410.

[37]. Hillborg H, Gedde UW, Polymer 1998, 39, 1991.

[38]. Bausch GG, Stasser JL, Tonge JS, Owen MJ, Plasmas Polym. 1998, 3, 23.

[39]. Zhou J, Ellis AV, Voelcker NH, Electrophoresis 2010, 31, 2. [PubMed: 20039289]

[40]. Beal JH, Bubendorfer A, Kemmit T, Hoek I, Arnold WM, Biomicrofluidics 2012, 6, 036503.

[41]. Karakoy M, Gultepe E, Pandey S, Khashab MA, Gracias DH, Appl. Surf. Sci 2014, 30, 684.

[42]. Zhang Z, Wang J, Tu Q, Nie N, Sha J, Liu W, Liu R, Zhang Y, Wang J, Colloids Surf., B 2011, 88, 85.

[43]. Merkel TC, Bondar VI, Nagai K, Freeman BD, Pinnau I, J. Polym. Sci., Part B: Polym. Phys 2000, 38, 415.

[44]. Nicolle L, Antimicrob. Resist. Infect. Control 2014, 3, 23. [PubMed: 25075308]

[45]. Feneley RCL, Hopley IB, Wells PNT, J. Med. Eng. Technol 2015, 39, 459. [PubMed: 26383168]

[46]. Miranda I, Souza A, Sousa P, Ribeiro J, Castanheira EMS, Lima R, Minas G, J. Funct. Biomater 2021, 13, 2. [PubMed: 35076525]

[47]. Almany L, Seliktar D, Biomaterials 2005, 26, 2467. [PubMed: 15585249]

[48]. Cai S, Wu C, Yang W, Liang W, Yu H, Liu L, Nanotechnol. Rev 2020, 9, 971.

[49]. Zhou J, Khodakov DA, Ellis AV, Voelcker NH, Electrophoresis 2011, 33, 89. [PubMed: 22128067]

[50]. Gökaltun A, Kang YB, Yarmush ML, Usta OB, Asatekin A, Sci. Rep 2019, 9, 1. [PubMed: 30626917]

[51]. Mukhopadhyay R, Anal. Chem 2005, 77, 429 A.

[52]. Xu W, Flores-Mireles AL, Cusumano ZT, Takagi E, Hultgren SJ, Caparon MG, npj Biofilms Microbiomes 2017, 3, 28. [PubMed: 29134108]

[53]. Walker JN, Flores-Mireles AL, Pinkner CL, Schreiber HL, Joens MS, Park AM, Potretzke AM, Bauman TM, Pinkner JS, Fitzpatrick JAJ, Desai A, Caparon MG, Hultgren SJ, Proc. Natl. Acad. Sci. USA 2017, 114, E8721. [PubMed: 28973850]

[54]. Flores-Mireles AL, Walker JN, Bauman TM, Potretzke AM, Schreiber HL, Park AM, Pinkner JS, Caparon MG, Hultgren SJ, Desai A, J. Urol 2016, 196, 416. [PubMed: 26827873]

[55]. Baskin JL, Pui C-H, Reiss U, Wilimas JA, Metzger ML, Ribeiro RC, Howard SC, Lancet 2009, 374, 159. [PubMed: 19595350]

[56]. Kuter DJ, Oncologist 2004, 9, 207. [PubMed: 15047925]

[57]. Geerts W, Hematol. Am. Soc. Hematol. Educ. Program 2014, 1, 306.

[58]. Shao Q, Jiang S, Adv. Mater 2014, 27, 15. [PubMed: 25367090]

[59]. Habash M, Reid G, J. Clin. Pharmacol 1999, 39, 887. [PubMed: 10471979]

[60]. Chang TY, Yadav VG, De Leo S, Mohedas A, Rajalingam B, Chen C-L, Selvarasah S, Dokmeci MR, Khademhosseini A, Langmuir 2007, 23, 11718. [PubMed: 17915896]

[61]. Gnanasakthy A, Barrett A, Norcross L, D'Alessio D, Romano C, Value Health 2021, 24, 1016. [PubMed: 34243825]

[62]. Kamper SJ, Maher CG, Mackay G, Man J. Manipulative Ther. 2009, 17, 163.

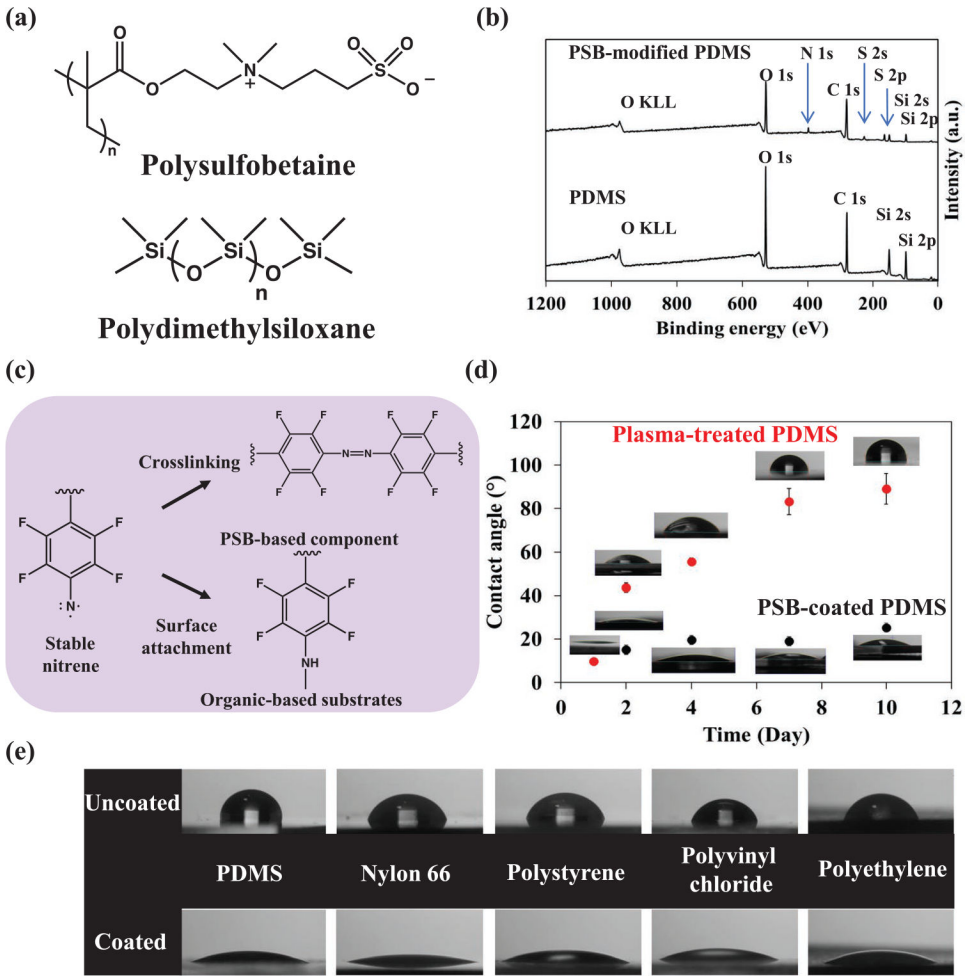

Figure 1.

Facile one-step surface modification of organic-based substrates with antibiofouling zwitterionic PFPA-PSB. a) Chemical structure of PFPA-PSB composed of zwitterionic PSB-based and UV-light reactive PFPA-based components. b) XPS spectra of a PSB-modified PDMS substrate showing the successful anchoring of PFPA-PSB on a silicone-based organic substrate (PDMS). c) PFPA-PSB undergoes self-cross-linking and binds to organic-based substrates upon UV exposure. d) Evolution of water contact angle on PDMS substrates treated with O_2 plasma (red symbols) and with the PSB treatment (black symbols). The plasma-treated substrate exhibits rapid hydrophobic recovery, whereas the PSB-modified substrate remains hydrophilic for an extended period. e) PFPA-PSB is able to coat a wide spectrum of organic-based substrates, including PDMS, nylon 66, polystyrene, polyvinyl chloride, and polyethylene, imparting robust hydrophilicity to them via a facile UV light-mediated molecular anchoring mechanism. These substrates have been commonly used in a variety of industrial applications, such as biomedical devices.

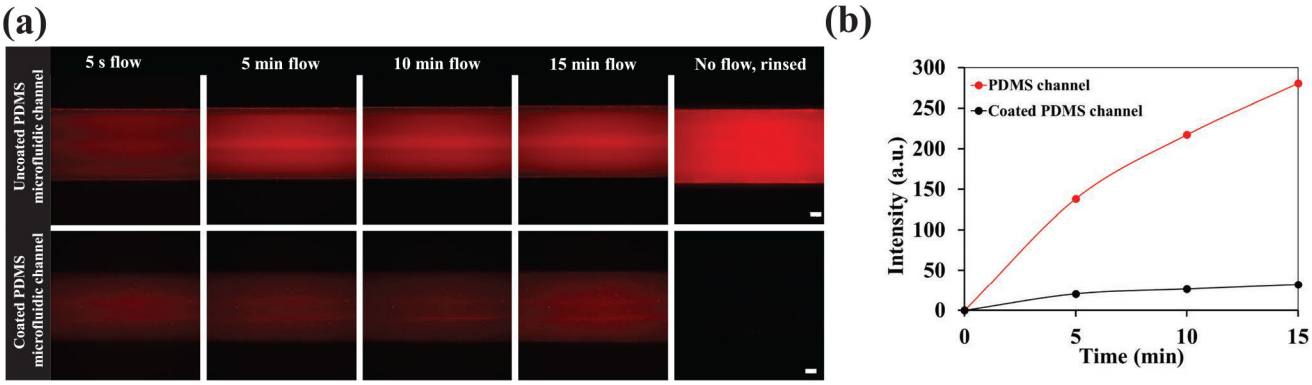

Figure 2.

Protein adsorption on PFPA-PSB-coated substrates. a) Fluorescent images of Alexa Fluor 546-conjugated fibrinogen flow in uncoated and PSB-coated PDMS microfluidic channels. b) Quantification of fibrinogen adsorption to PDMS microfluidic channels under flow.

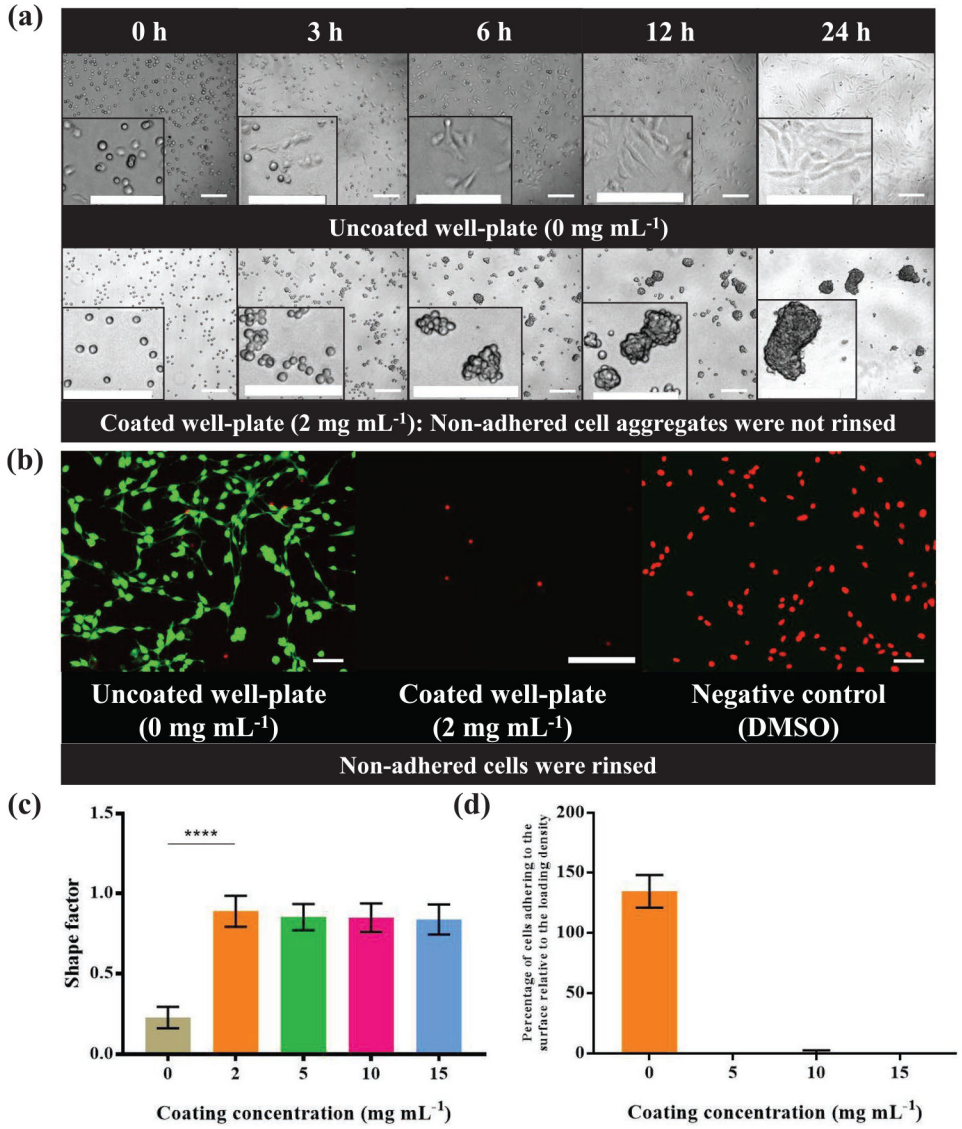

Figure 3.

Assessment of cell adhesion on PFPA-PSB-coated cell culture well plates. a) Bright field images of NIH/3T3 fibroblast monolayer culture 0, 3, 6, 12, and 24 h post seeding on 96-well plates. The upper panel presents the cell behavior on unmodified substrates, indicating cell spreading initiated within ≈3 h post seeding. After ≈6 h, most of the cells were adhered and elongated on the unmodified substrate. In contrast, the PSB-coated substrates did not permit cell adhesion, maintaining the cells in suspension, which resulted in cell aggregation within a few hours post seeding. b) Live/dead staining of fibroblast cells after 24 h culture on the unmodified substrates shows that the cells adhered to the unmodified substrate and remained viable; however, no live cells were observed on the PSB-coated substrates due to the lack of adhesion. The negative control shows that all the adhered cells were dead in DMSO. c) The shape factor of cells 24 h post seeding defined as $4\pi A/P^2$, where A is the cell surface area and P is the perimeter. This factor is a measure of spreading (elongation) tendency, which shows that the cells cultured on the unmodified substrates

undergo spreading (shape factors ≈ 0) and those cultured on the PSB-coated substrates are almost spherical (shape factors ≈ 1). d) The percent of cells adhered to unmodified substrates, showing the proliferation of adhered cells in 24 h, is compared with almost no cell attachment on the PSB-modified substrates. Scale bars in (a) and (b) are 200 and 100 μm, respectively.

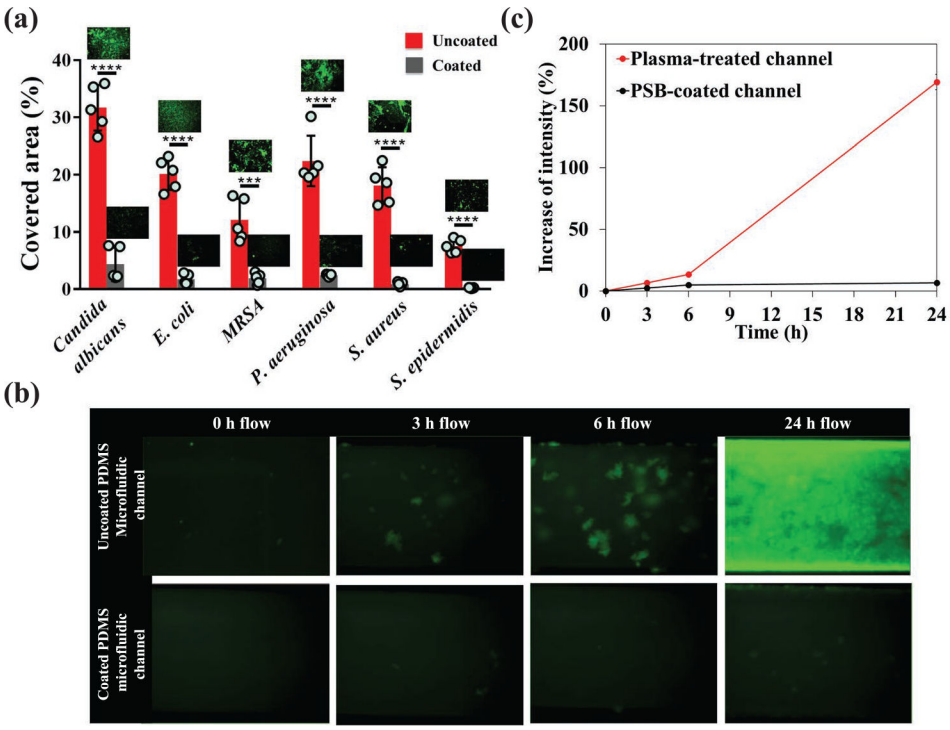

Figure 4.

Assessment of microbial (bacterial and fungal) adhesion to PFPA-PSB-coated PDMS substrates. a) Percentage of fungal and bacterial cell coverage on bare and PSB-coated PDMS substrates obtained from representative fluorescent microscopy images (insets). b) Adsorption of fluorescent *E. coli* (ATCC 25922GFP) to PDMS microfluidic channels under flow within 24 h shows that the uncoated channels permitted full coverage, whereas the PSB-coated channels did not support bacterial adhesion. The scale bars represent 100 μm. c) Increase of intensity over time based on the quantification of fluorescent images in (b) shows that while uncoated channels underwent more than 160% increase in intensity in 15 min as a result of bacterial deposition, the coated channels remained protected against the bacterial adhesion.

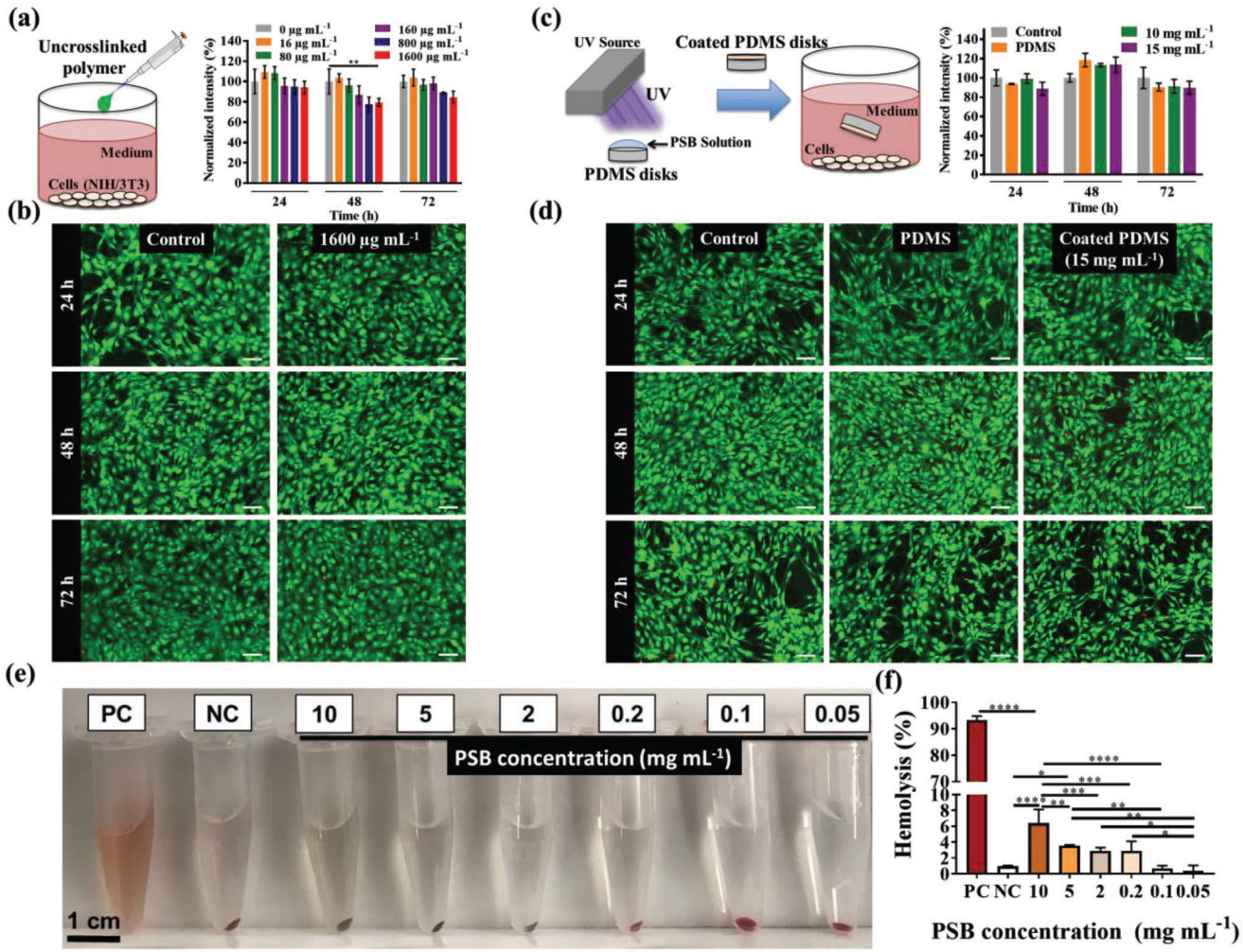

Figure 5.

Assessment of the cytotoxicity and hemolysis of PFPA-PSB. a) Assessing the cytotoxicity of uncross-linked PSB by adding a desirable amount of the polymer to the cell culture media of cultured monolayer NIH/3T3 fibroblast cells and measuring the metabolic activity of cells using the MTT assay. Fluorescent intensity shows that the cells, regardless of the PSB concentration (up to 1600 μg mL^{-1}) are able to metabolize the cell membrane-permeable tetrazolium dye MTT, which attests to the insignificant effect of PSB on the cell viability. b) Live/dead staining of the monolayer fibroblast cells cultured in the presence of uncross-linked PSB shows a 100% viability of cells within 72 h. The controls show the cells cultured in the absence of PSB. c) The cytotoxicity of cross-linked PSB was investigated by applying the treatment on PDMS discs, followed by incubating the discs in the cell culture media of cultured monolayer fibroblast cells. The metabolic activity of the cells does not show any significant difference with the PSB-free control. d) Live/dead staining of the fibroblast cells cultured in the presence of cross-linked PSB shows that almost no cell is compromised compared to the PSB-free controls. e) Effect of uncross-linked PSB on the RBCs, shown by the optical images of Eppendorf tubes containing varying concentrations of PFPA-PSB in heparinized human whole blood after centrifuging from which f) the hemolysis percentage

of RBCs are calculated. Compared to the positive control (PC, Triton X-100), the uncross-linked PFPA-PSB results in ≤6% hemolysis at ≤10 mg mL^{-1}. Accordingly, uncross-linked and cross-linked PSB are both nontoxic for the cells, rendering this material suitable for coating medical devices that are in contact with cells.